

A Phantom Designed Specifically for Local SAR Validation

Matthew Restivo¹, Ronald Mooiweer¹, C.A.T van den Berg¹, Alexander Raaijmakers¹, Frank Simonis¹, Peter Luijten¹, and Hans Hoogduin¹
¹University Medical Center Utrecht, Utrecht, Netherlands

Introduction: SAR safety is an important issue for 7T MRI as localized SAR hot spots can potentially result in dangerous heating.¹ Safety decisions for peak local SAR must rely on numerical electromagnetic simulations of RF coil models loaded with human body models. However, prior to this SAR assessment it is important to obtain confidence in the coil models by validation using phantom experiments. Phantoms are typically dielectrically homogenous and therefore do not exhibit very localized heating. We built a phantom which exhibits significant localized heating and provides good conditions for measuring temperature rise with MR thermometry and/or using fiber optic temperature probes.

Methods: The phantom design consists of four 1 cm diameter tubes that run longitudinally through a 15 cm diameter cylinder, all made from PMMA (Fig. 1). The tubes are filled with a saline gel with a conductivity of 2.4 S/m at 298 MHz (measured using an Agilent 85070E dielectric probe). This is similar to the highest conductivity seen in a human head at 7T (CSF=2.2 S/m). Two of the tubes are narrowed to .5 cm diameter in the center so that current, and thus SAR, will be concentrated in that region (Fig.2). The larger cylinder is filled with oil. The oil is important in the phantom because it has near zero conductivity and will minimally heat with application of RF energy. Also, oil does not have a temperature dependent proton resonant frequency shift (PRFS), which allows us to use the phase change in the oil for field drift correction enabling more accurate PRFS thermometry.² Validation experiments were performed using a quadrature birdcage head coil. Proton Resonance Frequency Shift (PRFS) MR thermometry was performed using an FFE sequence with the addition of a high power pre-pulse every TR (455° flip angle at 10 kHz frequency offset to cause heating but not affect the MR image). The MR thermometry was performed using a 10° flip angle, TR=22ms, TE = 15ms, and minimal water-fat shift. The sequence was repeated consecutively 16 times for a total duration of 5 minutes.

The SAR distribution was simulated using Semcad X (Speag AG, CH). Additionally, the Semcad thermo-solver, based on Pennes bioheat model, was used to simulate the temperature rise due to five minutes of heating. Temperature simulations were normalized to the same power used in MR experiments by comparing measured and simulated B1+.

Experiments were done with the phantom in two different positions. The first position was with the phantom centered in the longitudinal center of the coil, but 1.5 cm up from isocenter, so that the electric field would not be symmetric and uneven heating would occur. In the second position, the center of the phantom was moved to the longitudinal edge of the coil and rotated 90° with respect to position 1. This position was chosen because the birdcage produces higher electric fields near the edge of the coil compared to the center, and therefore should produce more heating. In previous experiments using this phantom, MR thermometry results have shown good agreement with fiber optic temperature probes inserted directly into the tubes. For this particular study, temperature probes were omitted because they are not included in simulations.

Results: The simulated peak 1g averaged SAR is $1.60 \text{ W} \cdot \text{kg}^{-1} \cdot \mu\text{T}^{-2}$ in position 1 when normalized to the average B1+ over the axial slice in the center of the coil. SAR1g increases to $2.80 \text{ W} \cdot \text{kg}^{-1} \cdot \mu\text{T}^{-2}$ when the phantom is moved to position 2. For comparison, the SAR1g in the head of a human model (Duke of the Virtual Family³) using the same coil is $2.61 \text{ W} \cdot \text{kg}^{-1} \cdot \mu\text{T}^{-2}$. Fig. 3 shows the maximum temperature rise observed using MR thermometry compared to the simulated SAR distribution for both positions. Fig. 4 shows the temperature rise measured by thermometry over time compared to the temperature rise expected from simulations at the center of each of the four tubes with the phantom at position 1. Maximum temp rise measured was $\approx 1.4^\circ\text{C}$ vs. maximum temp rise simulated was $\approx 1.3^\circ\text{C}$. Much more heating was measured at position 2, where maximum temp rise measured was $\approx 5^\circ\text{C}$ vs. maximum temp rise simulated was $\approx 3.4^\circ\text{C}$.

Discussion: Thermometry measurements for two different positions show reasonable agreement with temperature simulations. As expected, a larger temperature rise is observed in the narrowed tubes compared to the straight tubes. While the overall temperature difference is dependent on local SAR in the tubes as well as thermal effects (e.g. heat conductions), the initial slope of the temperature rise is directly indicative of the local SAR. The time course of heating in Fig. 3 shows that the initial slope of the temperature rise is predicted accurately by the simulation. Thus, there appears to be a match between actual and predicted local SAR levels. The most likely source of error in the simulations is positioning of the model with respect to the coil. The birdcage coil generates an electric field distribution that is strongly inhomogeneous. Small changes in position lead to large changes in electric field intensity within the conductive tubes. In the tube with the highest observed heating (Fig. 3, Tube A, Pos. 2), simulations underestimate heating by 1.6°C (5°C measured vs. 3.4°C simulated). More experiments must be done in similar high-heating situations to confirm whether this is an error related to model positioning, thermal properties, or a different cause.

Conclusion: A phantom has been constructed that exhibits high localized SAR, which is comparable to peak local SAR in the human head during 7T MRI. The local SAR in this phantom can be measured by means of temperature rise using PRFS thermometry or directly using fiber optic probes inserted into the tubes. Measurements with this phantom allow for local SAR validation for RF coil models, a necessary step prior to relying on SAR simulations for in-vivo safety decisions.

References: 1) Neufeld et al, PMB, 2011;56 (15):4649-59. 2) Salomir et al, IEEE, 2012;31(2):287-301. 3) Christ et al, PMB, 2010;55:N23. *This work was supported by the Initial Training Network, HiMR, funded by the FP7 Marie Curie Actions of the European Commission (FP7-PEOPLE-2012-ITN-316716)*

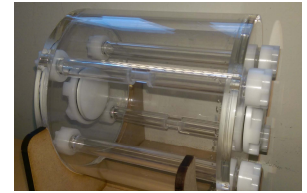


Figure 1: Photo showing the constructed phantom

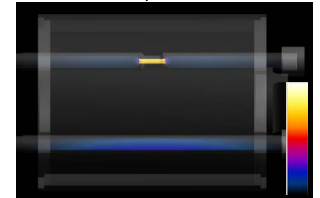


Figure 2: Sagittal view of simulated SAR distribution for the phantom in position 1. Very localized SAR is realized inside the narrowed tube compared to the straight tube

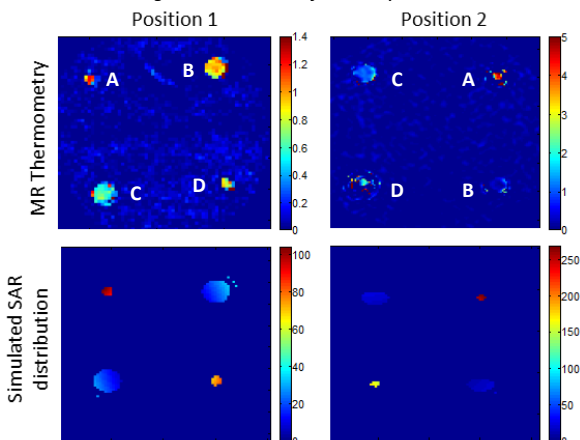


Figure 3: MR thermometry images show temperature rise in degrees Celsius over the center axial slice of the phantom after 5 min. Thermometry images show good agreement with simulated SAR distributions. SAR distributions are normalized to B1+ achieved in thermometry sequence. SAR has units of W/kg.

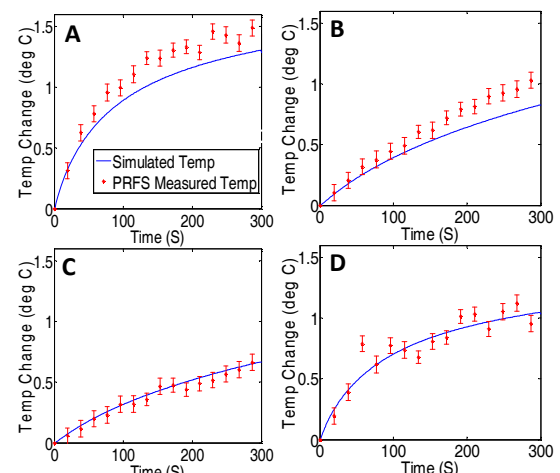


Figure 4: Simulated (blue) and measured (red) temperature rise over time in each of the four tubes (A-D) with the phantom placed in the center position (position 1). Error bars represent noise in the thermometry images computed from the standard deviation of temperature in an unheated region of the phantom.